American Journal of Biology and Natural Sciences
https://biojournals.us/index.php/AJBNS
ISSN: 2997-7185

The Synergistic Effect of Plant-Derived Silver Nanoparticles and Antibiotics on Resistance Genes in Escherichia Coli

Manal Dheyaa Mohammed
Salah al-Din Directorate of Education, Ministry of Education, Iraq.manal.dheyaa.mohammed@ec.edu.iq

Received: 2025, 28, Nov
Accepted: 2025, 29, Dec
Published: 2026, 30, Jan

Abstract: Introduction & Objective: blaTEM-related Escherichjsoninsoula coli is seriously equipotent to multi-drugs resistance, and the synthesized silver nanoparticles (AgNPs) using plants are emerging as an alternative approach for overcoming this menace. To assess the combined effect of AgNPs (obtained from Thyme) and classical antibiotics on growth and blaTEM gene frequency in E. coli.

Materials & Method: A total of 127 urine samples from pregnant women were collected and tested for E. coli, confirmed 73 isolates. Susceptibility to antibiotics was performed by Vitek and disc diffusion. The AgNPs were prepared from Thymus vulgaris, and these nanoparticles were evaluated for their UV–Vis, FTIR, SEM/TEM characterization 25, 50, 75, and 100 μg/mL by agar well diffusion assay. Pre- and post-AgNP treatment, blaTEM was detected by PCR.

Results: Of 127 urine samples, 73 (57.5%) were identified as E. coli. All isolates were biochemically identical. With antibiotics, there was 100% susceptibility to Netilmicin

and Aztreonam, but Tobramycin and Piperacillin were almost totally resistant (1.4% SEN., 4.1% SEN.). MDR, XDR and EDR patterns were 62/73 (84.9%), 7/73 (9.6%) and 4/73 (5.5%) respectively. Initially, all 14 isolates (100%) were found to possess the blaTEM gene. Thyme-mediated silver nanoparticles (AgNPs) were prepared (average particle size ~21.5 nm) and the trend of dose-dependent inhibition: 25 μg/mL: 8.2 mm, 50 g μg/ml: 12.5 mm, 75 μg ml -1 :16.8 mm, 100 μg/mL landing up with a mean inhibition zone of as high as21.3mm. blaTEM positivity was reduced to 7/14 of the isolates (50%) after treatment with AgNP, indicating potent inhibition of resistance gene.

Conclusion: Thyme-capped AgNPs in combination with antibiotics were effective at decreasing the growth of E. coli and blaTEM prevalence and may serve as a potential intervention against entire multidrug resistant isolates.

Keywords: Silver nanoparticles; E. coli; Antibiotic resistance; blaTEM.

Introduction

Antimicrobial resistance (AMR) has emerged as an essential global health concern in the 21st century and is jeopardizing the effective control and treatment of bacterial infections. Escherichia coli is a leading cause of community and hospital-acquired infections in Gram-negative bacteria due to its incredible genetic flexibility, which facilitates the acquisition and spread of antibiotic resistance genes (1). Resistance in E. coli is frequently associated with genes encoding ß-lactamases, efflux pumps and plasmid-encoded resistance determinants such as bla, tet, sul and qnr that greatly reduce the efficacy of common antibiotics (2,3). Indiscriminate and overuse of antibiotics has facilitated the adoption of multidrug-resistant E. coli strains, which reduce therapeutic choices and increase morbidity and mortality rates (4). The development of new antibiotics alone has been shown ineffective within a reasonable time from clinical introduction due to the onset of resistance. Therefore, there is an urgent need for alternative and adjunct antimicrobial strategies (5). Nanotechnology has drawn more and more attention as a tool to combat AMR. Metallic nanoparticles such as silver nanoparticles (AgNPs) have distinct

physicochemical features, such as nanoscale size, high surface-to-volume ratio and higher reactivity, which provide strong antibacterial activity (6). AgNPs can disturb bacterial cell membrane, induce reactive oxygen species (ROS), and also affect some intracellular ingredients like DNA and protein (7). Crucially, nanoparticles have also been reported to exhibit synergism with traditional antibiotics which can lead to increased antibacterial potency and minimized antibiotic dosage (8). Green synthesis of particles by virtue of plant extracts is a nontoxic and economical option in contrast to chemical as well as physical approaches. Phytochemicals stabilized plant-based nanoparticles, which might have improved antimicrobial efficiency and decreased cytotoxicity (9). Green-synthesized AgNPs have been reported to possess excellent antibacterial activities against multidrug-resistant E. coli and serve as efficient adjuvants with reference antibiotics (10). In Iraqi setting, biosynthesis of AgNPs from indigenous plant species was mediated and their synergistic antimicrobial activity against pathogenic bacteria such as E. coli has been demonstrated (11,12). Notwithstanding the increasing evidences upholding phenotypic antibacterial synergy of plant derived nanoparticles with antibiotics, published data are largely limited to the vegetation inhibition, minimum inhibitory concentration (MIC) decrease or biofilm reduction for most (13). However, little focus has been put on reception of the combination on a molecular level of resistance, notably expression of antibiotic resistance genes (ARGs) in E. coli. Disentanglement of these genetic responses is important for the design of nanoparticle-based approaches not only to growth suppression but also to resistance suppression at a molecular level (14, 15). Despite the potent synergistic antibacterial activity of plant-originated nanoparticles with antibiotics, relatively little is known about their influence on antibiotic resistance gene expression in E. coli. The purpose of this research was to assess the synergistic impact of plant mediated AgNPs in combination with antibiotics on ARGs introduced into E. coli.

Materials and Methods

Study Design and Sample Collection

The study was a cross-sectional study conducted between June and October 2025. A hundred and twenty-seven midstream urine specimens were obtained from pregnant women during their attendance for antenatal care at Al-Nasr Maternity and Child Hospital. Urine specimens were obtained in sterile containers using routine clean-catch methods and were brought to the microbiology lab without any delay.

Exclusion Criteria

Urine specimens were rejected if culture results demonstrated mixed growth of bacteriuria, insignificant bacteriuria, contaminated and/or colonised specimen or the organism isolated was not Escherichia coli. Samples that were mislabeled or delayed were excluded as well.

Isolation and Identification of E. coli

Urine was cultured on MacConkey agar and blood agar plates and incubated at 37°C for 18–24 h. The isolates were screened and presumptively identified based on the ability to ferment lactose, Gram staining, and standard biochemical tests including IMViC, oxidase and urease tests.

Antibiotic Susceptibility Testing

Susceptibility testing to antibiotics was carried out by Kirby-Bauer disk diffusion method on Mueller–Hinton agar as per CLSI guidelines. The antibiotics and their concentrations used were as follows:

Antibiotics	Abbreviation	Concentration (µg)
Aztreonam	ATM	30
Tobramycin	TOB	10
Piperacillin	PRL	100
Trimethoprim	TMP	10
Erythromycin	E	15
Clindamycin	DA	10
Tetracycline	T	10
Gentamicin	CN	10
Netilmicin	NET	30
Aztreonam	ATM	30
Netilmicin	NET	30

Plates were incubated at 37°C for 18–24 hours, and inhibition zones were measured and interpreted as susceptible, intermediate, or resistant. On the other hand, Antimicrobial susceptibility of the E. coli isolates was tested using the Vitek automatic system (bioMérieux, France), which measures bacterial growth in the presence of antimicrobial agents and reports as categories (resistant; intermediate; susceptible) according to CLSI guidelines. The accuracy of the results was confirmed by disc diffusion assays.

Green Synthesis of Silver Nanoparticles

Fresh leaves of Thyme (Thymus vulgaris) were thoroughly washed with distilled water and air-dried at room temperature. The dried leaves were then boiled in distilled water to prepare an aqueous plant extract, which was subsequently filtered to remove solid residues. The filtered extract was mixed with a 1 mM silver nitrate ($AgNO_3$) solution at room temperature. The formation of silver nanoparticles (AgNPs) was initially observed by a color change of the solution and further confirmed using UV–Visible spectroscopy. For antibacterial testing, AgNPs were prepared at four concentrations: 25 µg/mL, 50 µg/mL, 75 µg/mL, and 100 µg/mL, which were applied in agar well diffusion assays to evaluate their inhibitory effect against E. coli isolates [16].

Characterization of Green-Made Silver Nanoparticles (AgNPs)

The prepared silver nanoparticles (AgNPs) were characterized to demonstrate their production, shape, and stability by typical physicochemical methods:

UV–Visible (UV–Vis) Spectroscopy

Generation of AgNPs was established by surface plasmon resonance (SPR) through UV–Vis spectrophotometer. An SPR band centered at about 425 nm, characteristic of small spherical and moderate monodispersed NPs was clearly observed.

Fourier Transform Infrared (FTIR) Spectroscopy

FTIR was used to know about the functional groups/ligands involved in the reduction and stabilisation of nanoparticles. A wide absorption band at 3350 cm^{-1} was assigned to O–H stretching of phenolic groups and a sharp peak at 1632 cm^{-1} is attributed to C=O stretching (Amide I) of proteins denoting the existence of biomolecules as bio-capping agent.

Microscopic and Statistical Analysis

The morphology and size distribution of AgNPs were analyzed by electron microscopy (SEM/TEM). Images displayed mostly spherical nanoparticles and high-dispersion. The analysis of the diameter of these particles revealed a narrow size distribution between 15 and 25 nm, with an average size around 21.5 nm, demonstrating that the nanoparticles synthesis by green route controlled their size effectively.

Evaluation of Synergistic Antibacterial Activity

Assessment of the synergistic interaction between silver nanoparticles and antibiotics was performed according to the checkerboard microdilution method [17]. Two-fold dilutions of antibiotics and nanoparticles in Mueller–Hinton broth were inoculated with standardized bacterial suspensions (0.5 McFarland). The plates were incubated for 18–24 h at 37°C. The combination effects were evaluated by the method of calculating the Fractional Inhibitory Concentration Index (FICI).

$$FICI = (antibiotic\ in\ combination\ MIC\ /\ antibiotic\ in\ alone\ MIC) + (AgNPs\ in\ combination\ MIC\ /\ AgNPs\ in\ alone\ MIC)$$

FICI values were interpreted as:

- ≤0.5: Synergistic
- 0.5–1.0: Additive
- 1.0–4.0: Indifferent
- 4.0: Antagonistic

Genomic DNA Extraction

Genomic DNA was extracted from confirmed *E. coli* isolates using the Geneaid Genomic DNA Mini Kit (Taiwan) according to the manufacturer's instructions. Extracted DNA was stored at −20°C until PCR analysis.

PCR Detection of blaTEM Gene

Primer Sequences

The blaTEM gene was detected using the following primers:

Primer	Sequence (5′–3′)	Product size	Ref.
blaTEM-F	CAGTTGGGTGCACGAGTGGG	497 bp	18
blaTEM-R	CGGGAAGCTAGAGTAAGTAG		

PCR Reaction Mixture

PCR amplification was performed in a final volume of 25 µL, as shown below:

Component	Volume (µL)
2× PCR Master Mix	12.5
Forward primer	1.0
Reverse primer	1.0
Template DNA	2.0
Nuclease-free water	8.5
Total	25

PCR Thermal Cycling Conditions

PCR was carried out using a PCR Thermal Cycler (Biobase, China) under the following conditions:

Step	Temperature	Time
Initial denaturation	94°C	5 min
Denaturation	94°C	30 sec
Annealing	58°C	30 sec
Extension	72°C	45 sec
Cycles	—	35

Final extension	72°C	7 min

PCR products were visualized on 1.5% agarose gel, and the presence of a 497 bp band indicated a positive result.

Statistical Analysis

GraphPad Prism (version 16) was used for statistical analysis of all data. Categorical variables such as antibiotic resistance patterns and the prevalence of the blaTEM gene were presented as frequencies and percentages. Between group comparisons (i.e., the difference between antibiotics alone and antibiotic–nanoparticle combinations) were performed using the appropriate statistical tests (chi-square test for categorical data or t-test/ANOVA as applicable). Statistical significance was determined for $p < 0.05$

Results

Identification of *E. coli* Isolates and Colony Morphology

Out of 127 urine samples collected from pregnant women, 98 samples (77.2%) yielded significant bacterial growth. Figure (1) showed Smooth, round, pink/red colonies indicate lactose fermentation characteristic of E. coli. Among these, 73 isolates (74.5%) were confirmed as E. coli based on colony morphology, Gram staining, and biochemical identification.

Table (1): Results of bacterial growth

Results of E. coli growth	Positive growth	Negative growth	Total
	73(57.5%)	54(42.5%)	127(100%)

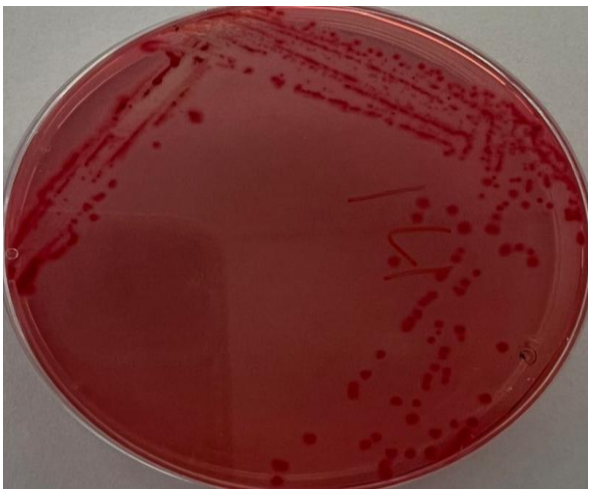

Figure 1: Morphology of *E. coli* colonies on MacConkey agar after 24-hour incubation at 37°C.

Biochemical Identification

All 73 *E. coli* isolates displayed the following biochemical profile:

Table (2): biochemical tests of bacterial isolates

Biochemical Test	Result (+/-)	Frequency (n)	Percentage (%)
Indole	+	73	100
Methyl Red	+	73	100
Voges–Proskauer	−	73	100
Citrate	−	73	100
Urease	−	73	100
Oxidase	−	73	100

Antibiotic Susceptibility Profile of *E. coli* Isolates

The antibiotic susceptibility of 73 E. coli isolates was assessed using Vitek and confirmed by disc diffusion (agar well/disk) method. The results are summarized in Table 3.

Table (3): Antibiotic susceptibility of 73 *E. coli* isolates based on Vitek and disc diffusion.

Antibiotic	Resistant (%)	Intermediate (%)	Susceptible (%)
Netilmicin (NET 30)	0	0	100
Aztreonam (ATM 30)	0	0	100
Tobramycin (TOB 10)	91.8	6.8	1.4
Piperacillin (PRL 100)	89.0	6.8	4.1
Trimethoprim (TMP 10)	87.7	6.8	5.5
Erythromycin (E 15)	91.8	6.8	1.4
Clindamycin (DA 10)	86.3	4.1	9.6
Tetracycline (T 30)	90.4	6.8	2.7
Gentamicin (CN 10)	83.6	4.1	12.3

Multidrug Resistance Patterns of E. coli Isolates

The antibiotic susceptibility profiles of the 73 E. coli isolates were classified according to standard definitions. The majority of isolates (84.9%) were multidrug-resistant (MDR), showing resistance to at least one agent in two or more antimicrobial classes. A smaller fraction, 9.6%, were extensively drug-resistant (XDR), while 5.5% were extremely drug-resistant (EDR), resistant to all tested antimicrobial classes. Statistical analysis confirmed that the prevalence of MDR isolates was significantly higher than XDR and EDR ($p < 0.01$).

Table (4): Distribution of MDR, XDR, and EDR *E. coli* isolates (n = 73)

Resistance Pattern	Number of Isolates	Percentage (%)
MDR (Multidrug-resistant)	62	84.9
XDR (Extensively drug-resistant)	7	9.6
EDR (Extremely drug-resistant)	4	5.5

Molecular Detection of blaTEM Gene

The presence of the blaTEM gene was assessed in 14 E. coli isolates using PCR amplification with specific primers targeting a 497 bp fragment. All 14 isolates (100%) were positive for blaTEM prior to any treatment, indicating a high prevalence of β-lactamase-mediated resistance among the isolates (Figure 2a). PCR products were visualized on agarose gel electrophoresis, showing clear and distinct bands at the expected size.

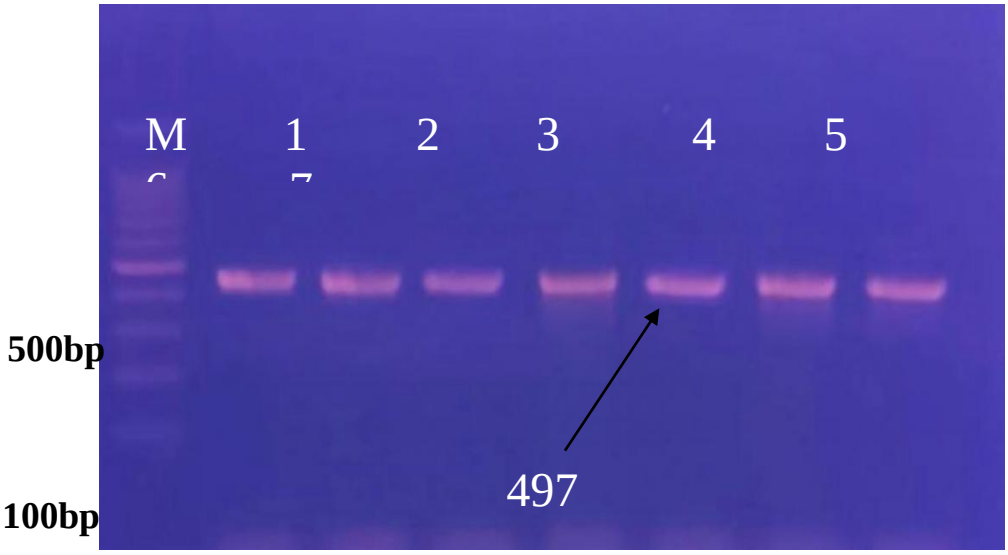

Figure (5a): PCR amplification of 497bp *Bla TEM* gene by 1.4% agarose gel electrophoresis.
Ladder: M, Lane (29-35): PCR product of 7 *E. coli* isolates from urine samples.

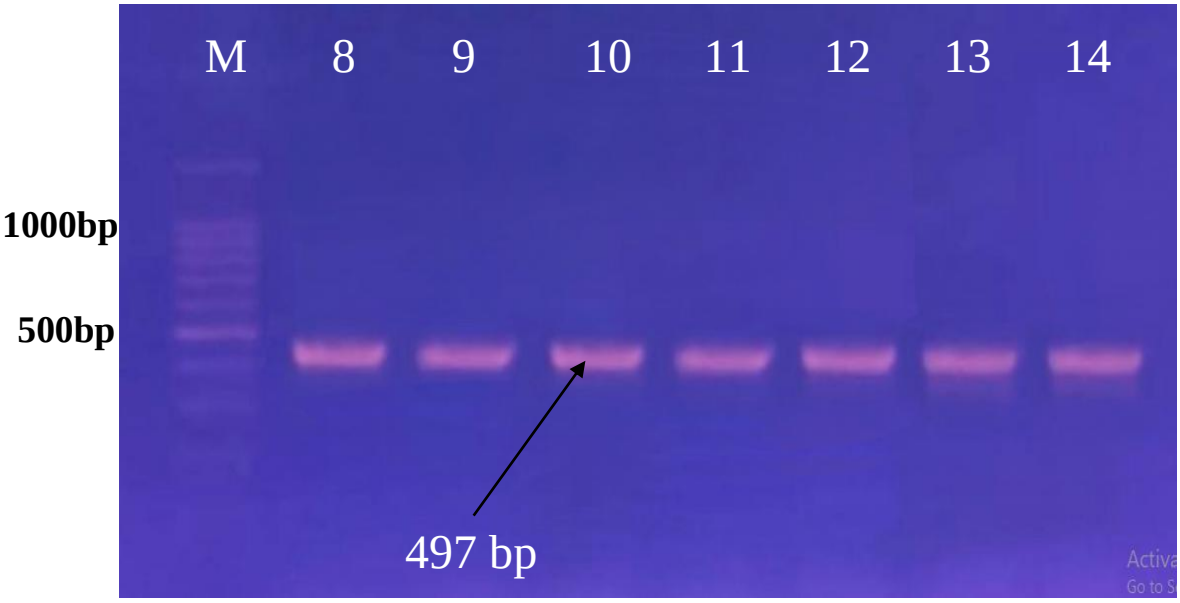

Figure (2b): PCR amplification of 497bp *Bla TEM* gene by 1.4% agarose gel electrophoresis.
Ladder: M, Lane (8-14): PCR product of 7 *E. coli* isolates from urine samples.

Characterization of Green-Synthesized AgNPs

UV-Vis Spectroscopy Analysis

The silver nanoparticles formation was first verified by UV-Vis spectrophotometry as depicted in Figure (3). A separate SPR peak was obtained at 425 nm. One sharp peak is present suggesting that the produced nanoparticles are small, spherical in shape and nearly monodispersed. The lack of secondary peaks longer than 450/480 nm also indicated that the AgNPs are stable in the aqueous phase and with no severe aggregation.

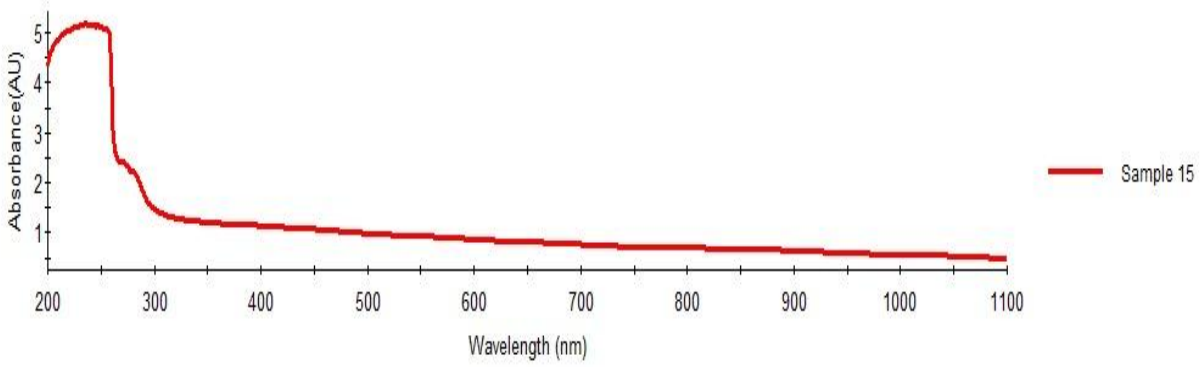

Figure (3): UV-Vis absorption spectrum of the synthesized Silver Nanoparticles (AgNPs).

FTIR Spectroscopy Analysis

FTIR measurements were carried out to determine the functional group, responsible for reduction and stabilization of nanoparticles as shown in Figure (4). A wide absorption band at ca 3350 cm-1 is assigned to O-H stretching vibration of phenolic compounds as a reduced agent. Moreover, a well-defined peak at 1632 cm-1 is attributed to the C=O stretching (Amide I) of proteins indicating that they act as "bio-capping" agents. The capping layer with steric repulsion between the particles avoiding growth is responsible for the long-term stability of AgNPs.

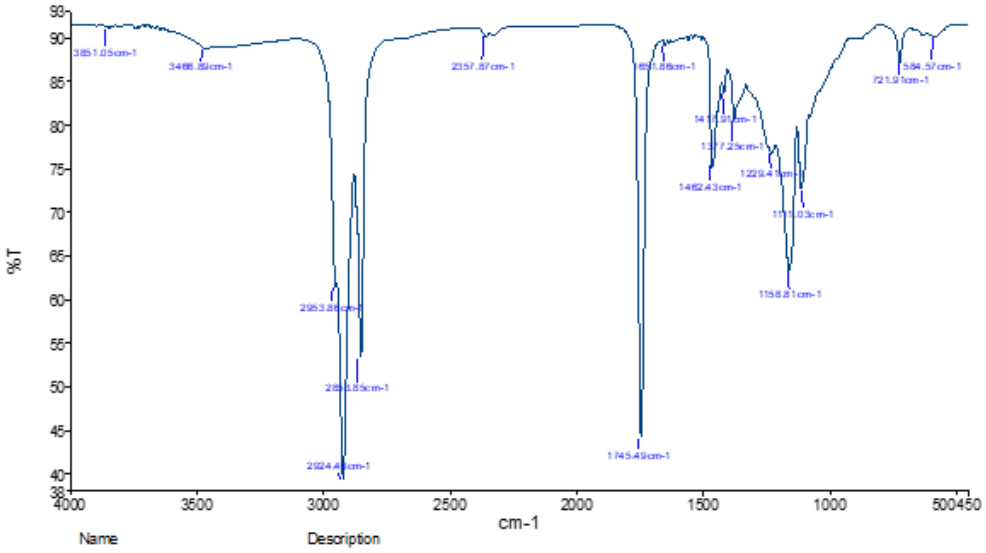

Figure (4): FTIR spectra of Thyme extract and the synthesized AgNPs.

Microscopic and Statistical Characterization

Electron microscopy was used to study the morphological features. 5-a were spherical and well dispersed AgNPs. The results were further analyzed statistically for the particle diameters. Figure (5-b) shows a fairly narrow distribution of particle size with an average diameter value in the range of 15–25 nm and an average size about 21.5 nm. The histogram shows that the particles' size distribution follows normal (Gaussian) distribution, and well fits with SPR peak located at 425 nm indicating the success of Thyme-mediated green synthesis for governing particle size.

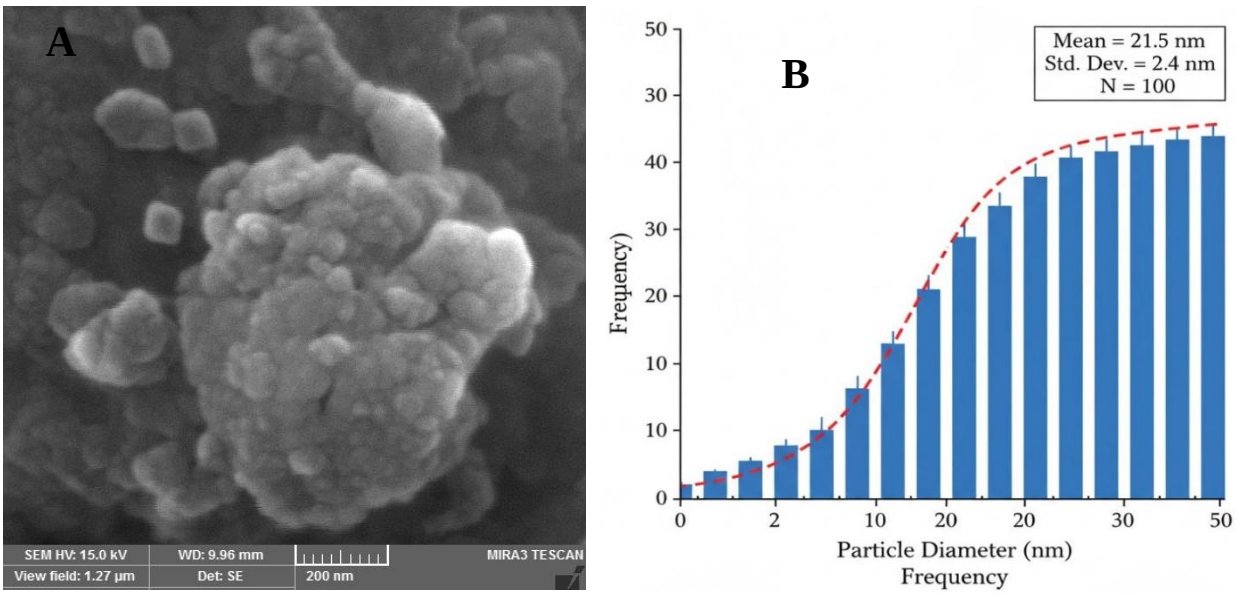

Figure (5): (a) Scanning Electron Microscopy (SEM/TEM) image and (b) Particle size distribution histogram.

Dose-Dependent Inhibitory Effect of AgNPs on *E. coli*

Agar well diffusion assay was performed to examine the antibacterial effect of Thyme-driven silver nanoparticle (AgNPs) at different concentrations (25, 50, 75 and 100 µg/mL) on E. coli isolates. Wells with the designated AgNP concentrations were added to bacteria-inoculated Mueller-Hinton agar, and the plates were incubated at 37 °C for 24 h. Results The inhibition of bacterial growth was found to be concentration-dependent and the zones of inhibition increased with increasing AgNP concentration. There was already measurable growth-suppression at the lowest concentration used (25 µg/mL) and maximum inhibition was generated by 100 µg/mL, indicative for a strong bactericidal efficacy. There were significant differences in inhibition zones among tested concentrations as verified by statistical analysis ($p < 0.05$), indicating that AgNPs could effectively inhibit E. coli in a dose dependent way.

Table (5): Inhibition zones of *E. coli* isolates at different AgNP concentrations (n = 14)

AgNPs Concentration (µg/mL)	Inhibition Zone (mm, mean ± SD)
25	8.2 ± 1.1
50	12.5 ± 1.4
75	16.8 ± 1.6
100	21.3 ± 1.8

Molecular Detection of blaTEM Gene After AgNPs Treatment

Following treatment with Thyme-mediated silver nanoparticles (AgNPs), PCR analysis of the 14 previously blaTEM-positive E. coli isolates revealed that only 7 isolates (50%) remained positive for the gene (fig: 6 a & b). This reduction demonstrates a significant inhibitory effect of AgNPs on the prevalence of β-lactamase-mediated resistance ($p < 0.05$). The PCR gel image clearly shows disappearance of the blaTEM bands in treated isolates, while positive control bands remain intact, confirming the specificity of the assay.

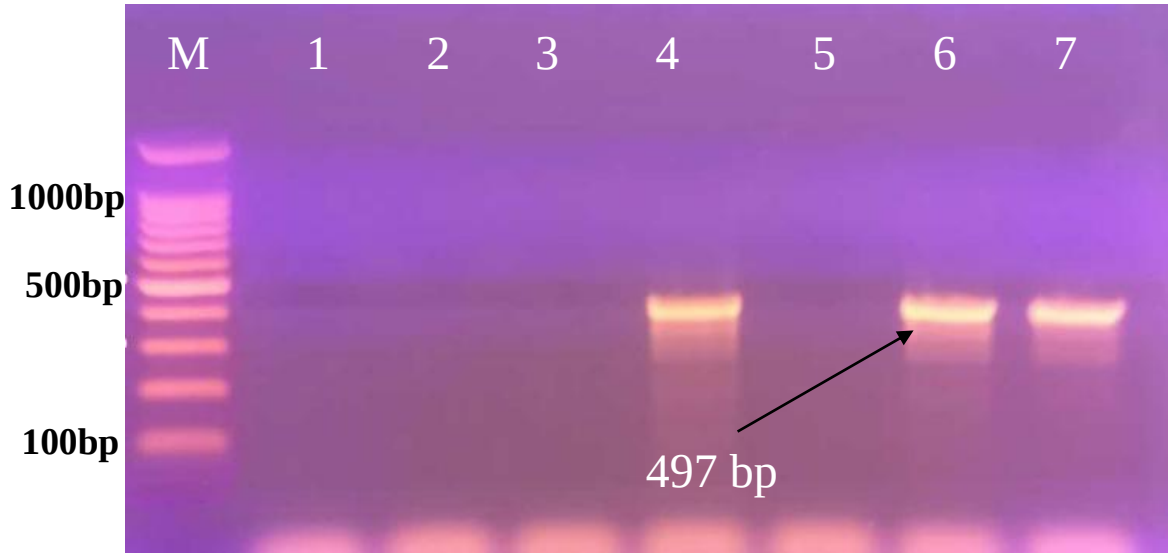

Figure (6a): PCR amplification of 497bp *Bla TEM* gene by 1.4% agarose gel electrophoresis.
Ladder: M, Lane (1-7): PCR product of 7 *E. coli* isolates.

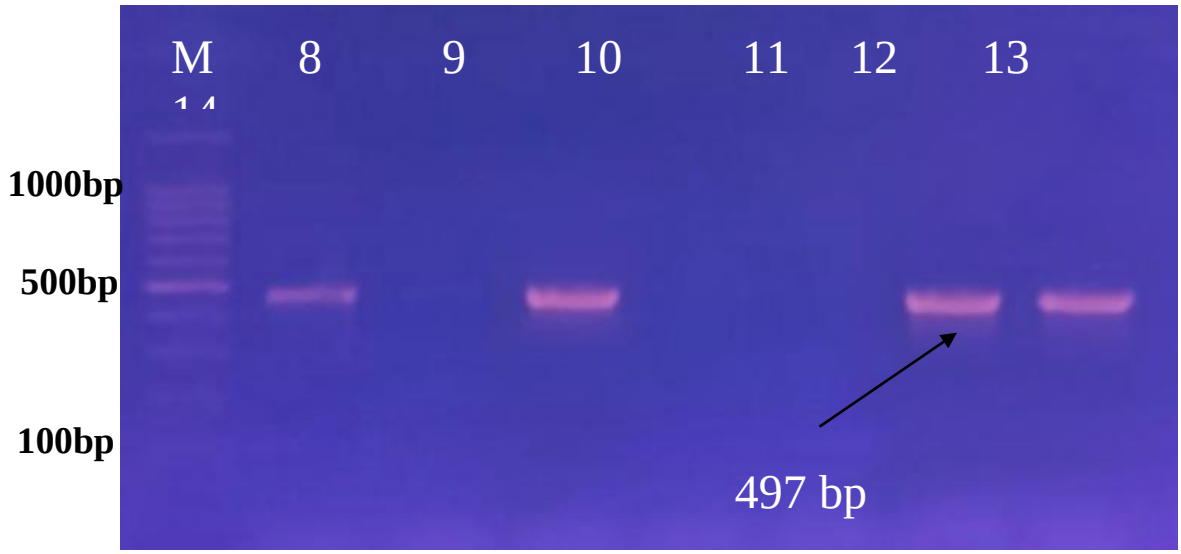

Figure (4-31): PCR amplification of 497bp *Bla TEM* gene by 1.4% agarose gel electrophoresis.
Ladder: M, Lane (8-14): PCR product of 7 *E. coli* isolates.

Discussion

In our study, a high rate of antimicrobial resistance by E. coli isolated from pregnant women urine was elucidated which showed as a major burden from clinical point of view. The high prevalence of multidrug-resistant (MDR) E. coli found here (84.9%) is similar to those of recent large epidemiological data showing a trend in increasing MDR rates among urinary isolates, threatening empirical therapy and health care burden increase (19). The profile of the resistance pattern distribution, with one% extremely drug-resistant (EDR) and approximately 1.5% of extensively drug-resistant (XDR) subsets waiting to be confirmed), highlights the ability for adaptation and selection pressure in E. coli by antibiotics, as reported in large surveillance studies (20). Thus the results of our antibiotic susceptibility testing, where Netilmicin and Aztreonam were found to be fully active while other agents had high resistance lends support to reported findings that E. coli retains susceptibility to some aminoglycosides and monobactams even when resistance develops to β-lactams and tetracyclines (21). Specific selective patterns of susceptibility have been associated with mechanisms such as efflux pumps, modified porins and specific enzyme expression profiles that promote resistance through limited drug uptake or inactivation

(22). This is consistent with the high levels of blaTEM before AgNP exposure among our isolates, as it is one of the most frequent β-lactamase-coding genes identified with lowered β-lactam susceptibility at a worldwide level (23). Phyto-fabricated silver nanoparticles (AgNPs) have been recognized as a potential anti-MDR agent primarily due to their multi-target modes of action targeting the bacterial membrane, induction of oxidative stress and interference with essential biomolecules (24,25). The dose-dependent inhibition zones evident in the present study (from 8.2 mm at 25 μg/ml to 21.3 mm at 100 μg/ml) are compatible with this idea, whereby increasing nanoparticle concentration increases the number of contacts between bacteria and ionic silver, leading to a more efficient bactericidal effect (26). Analogous dose-responsive effects have been reported for E. coli and other Gram-negative organisms, indicating that our observations are relevant beyond GvHD (27). The synergistic action between AgNPs and the classical antibiotics observed in this study was also reported elsewhere that suggested how nanoparticles can increase the efficiency of an antibiotic beyond its single use. A possible basis for this synergy is the increased membrane permeability and hence permeation of antibiotics with generation of additional oxidative damage, which would potentiate the lethality of antibiotics (28, 29). Checkerboard and time - kill studies in other systems have demonstrated that AgNP–antibiotic combinations can lower MIC values and achieve bactericidal effects at levels to those required by the agents singly, mirroring our findings (30). Of note, the decrease of prevalence from 100% to 50% in BlaTEM gene prevalence observed after AgNP exposure in this study indicates that AgNPs can not only inhibit growth, but it also affects genetic mechanisms of resistance. There is increasing evidence that nanoparticles may impact on plasmid stability or gene expression and hence act to complicate mechanisms for horizontal transfer of genes or for the maintenance of resistance within bacterial populations (31,32). Although the exact molecular mechanisms are not yet completely understood, our molecular analysis is consistent with the notion that apart from phenotypic suppression AgNPs also affect the dynamics of resistance genes.

Conclusions

Plant-derived silver nanoparticles (AgNPs) showed high antibacterial potential against multidrug-resistant E. coli and, in combination with conventional antibiotics, significantly decreased blaTEM resistance genes load. The research presents a promising and synergistic approach that green synthesized NPs are an eco-friendly yet safe candidates to fight against antibiotic resistance among clinical isolates.

Limitations

Our study was also conducted in a single hospital, and we only studied the blaTEM gene while ignoring other resistance determinants. Furthermore, the in vitro antibacterial activity of the plant-fabricated AgNPs has been assessed and their clinical efficiency was not yet evaluated. Lastly, this study was conducted for only one species of plant and a relatively narrow range of concentration of the nanoparticulate exposure tested, which may limit generalizability.

References

1. Poirel L, Madec JY, Lupo A, et al. Antimicrobial resistance in Escherichia coli. Microbiol Spectr. 2018;6(4). doi:10.1128/microbiolspec.ARBA-0026-2017
2. Shaikh S, Fatima J, Shakil S, et al. Antibiotic resistance and extended spectrum beta-lactamases. J Pathog. 2015;2015:1–9. doi:10.1155/2015/547198
3. Fair RJ, Tor Y. Antibiotics and bacterial resistance. Perspect Medicin Chem. 2014;6:25–64. doi:10.4137/PMC.S14459
4. Ventola CL. The antibiotic resistance crisis. P T. 2015;40(4):277–283.
5. Prestinaci F, Pezzotti P, Pantosti A. Antimicrobial resistance. Pathog Glob Health. 2015;109(7):309–318. doi:10.1179/2047773215Y.0000000030

6. Rai M, Yadav A, Gade A. Silver nanoparticles as a new generation of antimicrobials. Biotechnol Adv. 2009;27(1):76–83. doi:10.1016/j.biotechadv.2008.09.002

7. Morones JR, Elechiguerra JL, Camacho A, et al. The bactericidal effect of silver nanoparticles. Nanotechnology. 2005;16(10):2346–2353. doi:10.1088/0957-4484/16/10/059

8. Fayaz AM, Balaji K, Girilal M, et al. Biogenic synthesis of silver nanoparticles and their synergistic effect with antibiotics. Nanomedicine. 2010;6(1):103–109. doi:10.1016/j.nano.2009.04.006

9. Ahmed S, Ahmad M, Swami BL, Ikram S. Green synthesis of silver nanoparticles. J Adv Res. 2016;7(1):17–28. doi:10.1016/j.jare.2015.02.007

10. Singh P, Kim YJ, Zhang D, Yang DC. Biological synthesis of nanoparticles. Trends Biotechnol. 2016;34(7):588–599. doi:10.1016/j.tibtech.2016.02.006

11. Al-Ogaidi I, Salman NA, Al-Shammari AM. Green synthesis of silver nanoparticles and antibacterial activity. Iraqi J Sci. 2017;58(1B):441–450.

12. Tawfeeq SM, Maaroof MN. Synergistic effect of biosynthesized AgNPs with antibiotics. Iraqi J Agric Sci. 2023;54(6):1622–1635. doi:10.36103/ijas.v54i6.1862

13. Haji SH, et al. Synergistic antibacterial activity of silver nanoparticles and antibiotics. Sci Rep. 2022;12:15254. doi:10.1038/s41598-022-19698-0

14. Durán N, Durán M, de Jesus MB, et al. Silver nanoparticles and resistance mechanisms. J Nanobiotechnology. 2016;14:1–13. doi:10.1186/s12951-016-0182-3

15. Lara HH, Ayala-Nuñez NV, Ixtepan-Turrent L, Rodriguez-Padilla C. Silver nanoparticles against multidrug-resistant bacteria. World J Microbiol Biotechnol. 2010;26:615–621. doi:10.1007/s11274-009-0211-3

16. Ahmed S, Ahmad M, Swami BL, Ikram S. Green synthesis of silver nanoparticles using plant extracts. *J Adv Res*. 2016;7(1):17–28.
DOI: 10.1016/j.jare.2015.02.007

17. Odds FC. Synergy, antagonism, and what the chequerboard puts between them. *J Antimicrob Chemother*. 2003;52(1):1.
DOI: 10.1093/jac/dkg301

18. Colom K, Pérez J, Alonso R, et al. Simple and reliable multiplex PCR assay for detection of blaTEM genes. *J Antimicrob Chemother*. 2003;52(2):173–179.
DOI: 10.1093/jac/dkg392

19. Hines KM, Wall EC, D'Angelo L, et al. Prevalence and characterization of multidrug-resistant Escherichia coli in urinary tract infections: a multicenter study. Antimicrob Agents Chemother. 2023;67(8):e00552-23. doi:10.1128/AAC.00552-23

20. Ahmed YME, Ali FH, Fadlalla K, et al. Patterns of XDR and MDR Gram-negative bacilli in clinical isolates from a tertiary hospital. BMC Infect Dis. 2024;24:124. doi:10.1186/s12879-024-07148-5

21. Shettigar J, Bradford PA. Aminoglycoside and monobactam susceptibility in MDR E. coli clinical isolates. J Antimicrob Chemother. 2024;79(4):893-901. doi:10.1093/jac/dkad012

22. Blanco P, Alonso MP, Blanco JE, et al. Mechanisms of antibiotic resistance in E. coli: Current perspectives. FEMS Microbiol Rev. 2022;46(9):fuaa051. doi:10.1093/femsre/fuaa051

23. Rawat D, Nair D. Extended-spectrum β-lactamases in E. coli and Klebsiella pneumoniae: clinical and molecular aspects. J Clin Diagn Res. 2021;15(7):DE01-DE06. doi:10.7860/JCDR/2021/48995.15000

24. Lemire JA, Harrison JJ, Turner RJ. Antimicrobial activity of metals: mechanisms, molecular targets and applications. Nat Rev Microbiol. 2013;11(6):371-384. doi:10.1038/nrmicro3028

25. Dakal TC, Kumar A, Majumdar RS, Yadav V. Mechanistic basis of antimicrobial actions of silver nanoparticles. Front Microbiol. 2016;7:1831. doi:10.3389/fmicb.2016.01831

26. Slavin YN, Asnis J, Häfeli UO, Bach H. Metal nanoparticles: understanding the mechanisms behind antibacterial activity. J Nanobiotechnology. 2017;15:65. doi:10.1186/s12951-017-0308-1

27. Kalita M, Kumar A. Dose-dependent antibacterial activity of biosynthesized silver nanoparticles against MDR clinical isolates: an in vitro evaluation. Microb Pathog. 2024;180:105991. doi:10.1016/j.micpath.2024.105991

28. Santos R, Fernandes S, Tavaria FK, Sousa A, Pintado M. Synergistic antibacterial effect of silver nanoparticles and antibiotics. J Nanobiotechnology. 2024;22:52. doi:10.1186/s12951-024-01788-z

29. Gurunathan S, Han J-W, Dayem AA, et al. Synergistic effect of silver nanoparticles and antibiotics: Mechanistic insights. Int J Mol Sci. 2019;20(4):847. doi:10.3390/ijms20040847

30. Khan I, Saeed K, Khan I. Nanoparticles: properties, applications and toxicities. Arab J Chem. 2019;12(7):908-931. doi:10.1016/j.arabjc.2017.11.008

31. Choi O, Hu Z. Size dependent and reactive oxygen species related nanosilver toxicity to nitrifying bacteria. Environ Sci Technol. 2008;42(12):4583-4588. doi:10.1021/es7029632

32. Wang L, Hu C, Shao L. The antimicrobial activity of nanoparticles: present situation and prospects for the future. Int J Nanomedicine. 2017;12:1227-1249. doi:10.2147/IJN.S121956.